OPEN ACCESS

University of BRISTOL

Szalai, R., Epp, B., Champneys, A. R., & Homer, M. E. (2010). On time-delayed and feed-forward transmission line models of the cochlea.

Link to publication record in Explore Bristol Research
PDF-document

ON TIME-DELAYED AND FEED-FORWARD TRANSMISSION LINE MODELS OF THE COCHLEA

ROBERT SZALAI[1], BASTIAN EPP[2], ALAN R. CHAMPNEYS[3] AND MARTIN HOMER[4]

ABSTRACT. The mammalian cochlea is a remarkable organ that is able to provide up to 60dB amplification of low amplitude sound with sharp tuning. It has been proposed that in order qualitatively to explain experimental data, models of the basilar membrane impedance must include an exponential term that represents a delayed feedback. There are also models that include, e.g., a spatial feed-forward mechanism, whose solution is often approximated by replacing the feed-forward term by an exponential term that yields similar qualitatively accurate results. This suggests a mathematical equivalence between time delay and the spatial feed-forward models. Using a WKB approximation to compare numerical steady-state solutions, we show that there is no such simple equivalence. An investigation of the steady-state outputs shows that both models can display sharp tuning, but that the time-delay model requires negative damping for such an effect to occur. Conversely, the feed-forward model provides the most promising results with small positive damping. These results are extended by a careful stability analysis of both models. Here it is shown that whereas a small time delay can stabilize an unstable transmission-line model (with negative damping), that the feed-forward model is stable when the damping is positive. The techniques developed in the paper are directed towards a more comprehensive analysis of nonlinear models.

1. INTRODUCTION

Hearing in mammals occurs via a complicated mechanism, in which the key organ in is the cochlea. It responds to sound pressure waves in fluid that are coupled to sound pressure waves in the outside air through the ear drum and the middle ear. Essentially, the cochlea is the stage of the auditory pathway where mechanical vibration is transformed into neural signals, to be transmitted to the brain. It is capable of sensing a wide range of frequencies and amplitudes, with a great frequency and temporal resolution, see e.g. [11].

The cochlea is also active; that is, it amplifies vibration by 50-60dB for small amplitudes. The active process displays a so-called compressive nonlinearity in its input-output characteristic; that is, the amplification decreases as the input amplitude increases. Moreover, there is sharp frequency tuning, so that individual spatial locations along the cochlea amplify different input frequencies. In this paper, we shall not consider the effect of variation of input amplitude. We instead suppose that the stimuli are sufficiently small so as to, engage the cochlear amplifier in full.

Mathematical modeling of the physiology of the cochlea has a long history dating back to Helmholtz [9], who suggested that it contains an ensemble of resonators that are sensitive to different frequencies. As the anatomy of the cochlea (illustrated schematically in Figure 1.1) became better understood, it was discovered by Békésy [2] that the cochlea supports a traveling wave that is the result of the interaction between the fluid and the resonant structures in the organ of Corti. Since then, due to the pioneering work of Charles Steele, and others, over more than 35 years, passive models of the fluid-structure interaction have been proposed and embellished, see [23] and references therein. Many of the features of the fine tuning can be explained by the way
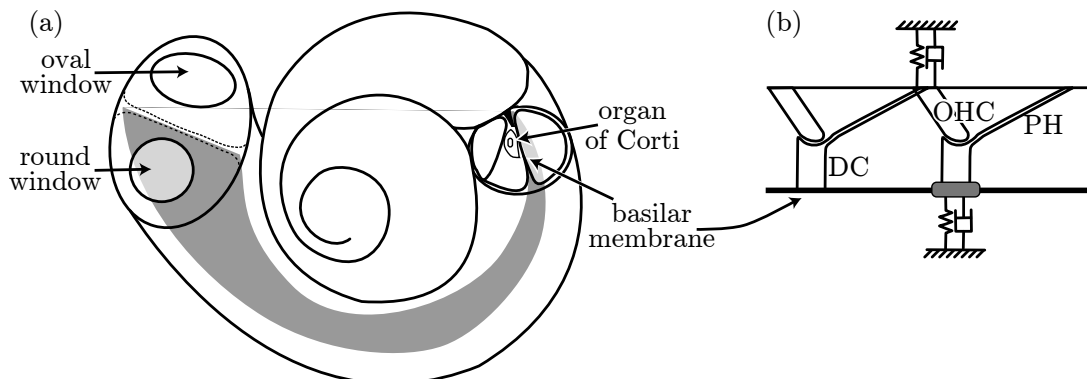
FIGURE 1.1. The basic anatomy of the mammalian cochlea. (a) The cochlea in its true representation as a coiled partitioned tube showing the basilar membrane as a shaded surface. (b) Longidudinal cross section of the organ of Corti, showing the basilar membrane, the phalangeal processes (PH) of the Deiter's cells and the tilted outer hair cells (OHC).

the geometry of the cochlear tube causes travelling waves to reach a maximum amplitude and stop at a frequency-dependent distance along the cochlea. More sophisticated cochlear models also exist, which take more detailed account of the fluid motion and the precise micro-mechanics of the cochlea based on physiological data, see e.g. [18, 17].

However, there are still significant questions to be answered, such as identifying the mechanism for amplification in the cochlea [4, 13]. It is widely held that outer hair cells are responsible for amplification but the mechanism is still unclear; see [1] for a discussion. In particular, two broad schools of thought suggest that either hair bundle motility [21] or the piezoelectric elongation of the cell body [3] are primarily responsible. Recent modeling studies suggest that a combination of the two mechanisms may be required in order to explain observed data [15, 20]. As a conceptual model of the active process, it has been proposed that the output at a fixed longitudinal position along the basilar membrane resembles that of a nonlinear oscillator that is tuned to be at the onset of a Hopf bifurcation [5].

One of the key unsolved problems associated with any active process is to explain how amplification can occur for very low inputs without activating an instability. In this paper we deal with feedback mechanisms in the cochlea that enhance tuning and provide the stability of the active process.

Another motivation for this work is the observation, due to Zweig [24], that most models of the cochlea cannot qualitatively fit measurement data for frequencies where the decay of the phase of the basilar membrane vibration becomes steep and then flat. In order to explain this inaccuracy, Zweig used a simple transmission line model and determined the impedance of the organ of Corti necessary to reproduce the experimental data. This extracted impedance implied that, in order to achieve a qualitative agreement with data, a delay term must be included in the transfer function of the organ of Corti. Zweig's results are striking, there is no obvious mechanism in the cochlea that can result in a pure time delay, independent of the dynamics.

Alternatively, there are other mechanisms that reproduce experimental data just as well, but do not explicitly include a time delay. Hubbard [10] introduced a secondary traveling wave that could be related to either the tunnel of Corti flow [12], or the waves of the tectorial membrane [8]. Also, tilting of the outer hair cells can introduce a spatial feed-forward mechanism that can

similarly explain experimental findings [7, 16]. However, not all mammalian species have tilting outer hair cells, but all have a phalangeal processes on their Deiter cells, resulting in logitudinal mechanical coupling (see Figure 1.1). Yoon and Steele argue that these processes, together with tilting outer hair cells lead to amplification via a push-pull mechanism [23].

The purpose of this paper is neither to resolve this controversy, nor to examine the physiological origins of any active process. Rather we shall use simple mathematical models to examine the generic effects on basilar membrane dynamics of coupling in both space and time, and the relationship between them.

The outline of the rest of this paper is as follows. In section 2 we introduce simple mathematical models of the cochlea described as a transmission-line. We describe models with time-delay and feed-forward longitudinal coupling. Further, we describe a solution technique that can determine the response of both models to oscillatory forcing, whether stable or unstable, and examine results with particular focus on the relationship between coupling in space and time. Section 3 then addresses the stability of the response of both models. Finally, section 4 draws conclusions and suggests avenues for future work.

2. Transmission line models

2A. **Zweig's model.** In the model introduced by [24], the cochlea is modeled as a rectangular box with two ducts of the same and constant cross-section A. The ducts are separated by the flexible basilar membrane, which is assumed in the model to have a single degree of freedom, with displacement $\xi(x,t)$, where x represents the longitudinal distance along the cochlea, measured from the stapes, and t time. The fluid in the ducts are driven by oscillations of the oval window that generate a pressure difference between the two ducts, $p(x,t)$ and drives the basilar membrane. The equations of motion can then be derived from the one-dimensional Stokes equation assuming that the endolymph/perilymph fluid inside the cochlea is inviscid and incompressible. The fluid mechanics can then be reduced to a single equation for the pressure difference $p(x,t)$ across the membrane:

$$\frac{\partial}{\partial t^2}p(x,t) = \frac{\varepsilon^2}{m}\frac{\partial}{\partial x^2}p(x,t), \tag{2-1}$$

where $\varepsilon^2 = \frac{2mA}{\rho\beta}$, m is the surface mass density of the basilar membrane, A is the cross section area of the duct, ρ is the fluid density and β is the width of the membrane. The relation between the pressure difference p and the basilar membrane displacement ξ is also determined by the mechanics of the basilar membrane, that is

$$\frac{p(x,t)}{m} = \frac{\partial}{\partial t^2}\xi(x,t) + 2\zeta(x)\omega_0(x)\frac{\partial}{\partial t}\xi(x,t) + \omega_0^2(x)\xi(x,t) + \sigma(x)\omega_0^2(x)\xi(x,t-\tau(x)). \tag{2-2}$$

The meaning of the parameters and space-dependent coefficients in Equations (2-1) and (2-2) are given in Table 2 along with the values that we have used in this study. Note that, apart from the damping factor ζ_0, which we allow to vary, these values are the same as those determined by Zweig in [24] and [6], where all distances are measured in the units of the uncoiled cochlea length. We will discuss the physiological motivation of the time-delayed feedback term below. Using the properties of linear equations one can assume that a steady time-periodic solution to the model (Equations (2-2) and (2-1)) can be expressed in the form of a series

$$p(x,t) = \sum_i \bar{p}_i(x)e^{\lambda_i t}, \tag{2-3}$$

Parameter	Value [Dimension]	Description
t	$t \in \mathbb{R}$ [ms]	Time
x	$0 \le x \le 1$ [-]	Longitudinal coordinate
ξ	- [-]	Membrane displacement
p	- [kg ms^{-2}]	Pressure difference
m	- [kg]	Membrane mass
A	- [-]	Duct cross-section
ρ	- [kg]	Fluid density
β	- [-]	Membrane width
$\theta(x)$	$e^{-10x} + e^{-20(1-x)}$ [-]	Interpolating function
$\zeta(x)$	$0.1e^{1.1973x}\theta(x) + \zeta_0 e^{-0.3914x}(1 - \theta(x))$ [-]	Relative damping factor
ζ_0	-0.06 or 0.01 [-]	Coefficient of $\zeta(x)$
$\omega_0(x)$	$\left(20.832e^{-4.8354x} - 0.1455\right) \times 2\pi$ [ms^{-1}]	Natural frequency of the membrane
$\sigma(x)$	$0.1416e^{-3914x}$ [-]	Feedback stiffness amplitude
ε	$\sqrt{\frac{2mA}{\rho\beta}} = 0.006$ [-]	Coupling parameter
$\tau(x)$	$1.742 \times 2\pi/\omega_0(x)$ [ms]	Feedback time delay

TABLE 2. Model parameters (Equation (2-4)).

which is a separation of variables with exponential time dependence and spatial patterns $\bar{p}_i(x)$. Substituting this expansion into Equations (2-3) and (2-1) we obtain

$$\lambda^2\bar{p} = \varepsilon^2\kappa^2(\lambda, x)\frac{\partial}{\partial x^2}\bar{p}, \qquad (2\text{-}4)$$

where

$$\kappa^2(\lambda, x) = \lambda^2 + 2\lambda\zeta(x)\omega_0(x) + \omega_0^2(x)\left(1 + \sigma(x)e^{-\lambda\tau(x)}.\right)$$

Equation (2-4) has to hold for each $\bar{p} = \bar{p}_i$ and $\lambda = \lambda_i$, where as yet we have not determined which values λ_i must take.

The natural boundary condition to take at apex of the cochlea, where fluid is allowed to flow between the two chambers divided by the basilar membrane, is

$$p(1, 0) = 0. \qquad (2\text{-}5)$$

Typically the choice of λ_i's is determined by the boundary condition at the stapes, which we assume to take the form $\frac{\partial}{\partial x}p(0, t) = -\rho v_{st}(t)$, where v_{st} is the stapes velocity.

In this study we shall assume a single frequency sound input with constant phase. It is most convenient to solve in complex co-ordinates, and therefore we set

$$\frac{\partial}{\partial x}p(0, t) = -\rho v_{st}(t) = e^{i\omega t}. \qquad (2\text{-}6)$$

The form of the boundary conditions, Equations (2-5) and (2-6), means that we can choose a single $\lambda = i\omega$ and a single $\bar{p}$ and hence the boundary conditions on $\bar{p}$ become

$$\frac{\partial}{\partial x}\bar{p}(0) = 1, \qquad \bar{p}(1) = 0. \qquad (2\text{-}7)$$

Hence we have reduced the dynamic problem to that of finding a steady solution to the two-point boundary value problem (2-4) for $\bar{p}(x)$ subject to the boundary conditions (2-7). In order

to solve such a problem we have used Chebyshev collocation [22] with 2400 mesh points in x, which yields very high accuracy.

A typical numerical solution for the excitation pattern of the cochlea, defined as the maximum amplitude of the basilar membrane at each longitudinal position x, is shown in Figure 2.1 for the particular choice of stimulus frequency 1.6kHz. Solutions with non-zero time delay are represented by continuous green lines, and without time-delay ($tau(x) = 0$) by dotted black lines. Similar results are obtained for a variety of different input frequencies with the sharp peak occurring at a frequency-dependent distance. It can be seen that with negative damping
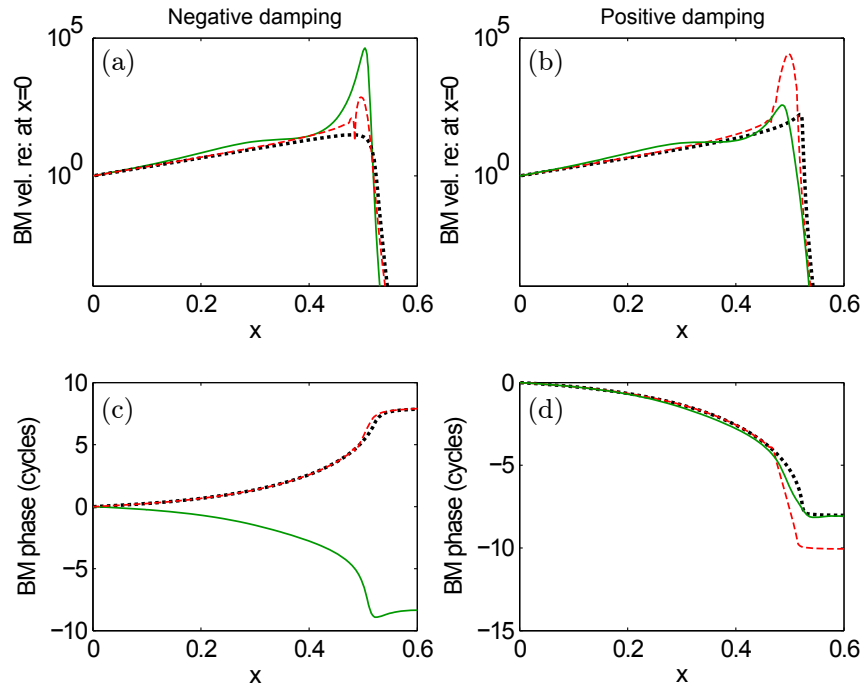

FIGURE 2.1. Steady state solutions of cochlea models for 1.6kHz harmonic stimulus: continuous green curves correspond to the time-delay model (2-4), dotted black lines correspond to the time-delay model with $\tau(x) = 0$, and dashed red lines corresponds to the feed-forward model (2-9). The damping parameter for the left column is $\zeta_0 = -0.06$, and for the right column is $\zeta_0 = 0.01$.

$\zeta_0 = -0.06$ (left-hand column of Figure 2.1), the tuning is sharper than with small positive damping ($\zeta_0 = 0.01$; right-hand column of Figure 2.1). We also can see that when the delay is removed there is no sharp tuning. Moreover, the phase curves (bottom row of Figure 2.1) suggest that the zero-delay case causes instability in the presence of negative damping, as the phase increases rather than decreases with x. Note that a decrease in phase is not a sufficient condition for stability, and a thorough stability analysis needs to be carried out to assess the stability. Such an analysis forms the subject of Section 3.

2B. **Delay equivalency.** It can be argued that time delay in the active part of the cochlea, although it cannot be directly related to a physiological effect, is in some sense equivalent to a spatial feed-forward mechanism that captures the action of the tilted hair cells and the phalangeal

processes. The logic for this argument is that the the cochlea supports a traveling wave whose speed is easily determined. From this speed, and starting from a time-delay model, one can calculate the distance that the wave travels during a fixed delay interval. This distance should then be equal to the spatial constant of the feed-forward mechanism.

The reason for studying the temporal delay model is that it is much simpler to solve using the method we introduced in the previous section, and the model with delay can can reproduce the cochlear response qualitatively better than without delay, as shown by the continuous green curves in Figure. 2.1. It is useful then to consider the relation between the time-delay and feed-forward models in more detail.

We use the WKB technique to solve Equation (2-4). The approximate solution assumes the form of $\bar{p}(x) = \sinh\phi(x)/\varepsilon$ with $\phi(x) = -\int_x^1 \frac{\lambda}{\kappa(\lambda,z)} dz$. The wavelength of the solution becomes

$$\delta(x) = \frac{2\pi\varepsilon}{\mathrm{Im}\left(\frac{i\omega_0(x)}{\kappa(i\omega_0(x),x)}\right)}.$$

With knowledge of the spatial wavelength, it is possible to calculate the distance that will have the same phase as the delayed wave, $\bar{p}(x)e^{-\lambda\tau}$, namely $\bar{p}(x + \Delta(x))$, where

$$\Delta(x) = \omega_0(x)\tau(x)\delta(x) \tag{2-8}$$

Note that since $\tau(x)\omega(x)$ is a constant, $\Delta(x)$ is a constant multiple of $\delta(x)$, and note further that $\delta(x)$ is roughly constant along the cochlea. For our parameter values, the estimated feed-forward distance $\Delta(x)$ defined by Equation (2-8) is plotted in Figure 2.2. The obtained distance values are unreasonably large, around 2% of the length of the uncoiled cochlea, which would mean 0.75mm for the 35mm long human cochlea.
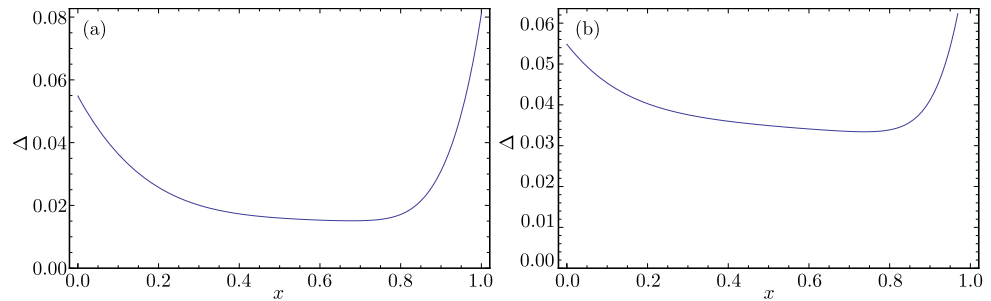

FIGURE 2.2. The equivalent feed-forward distance $\Delta(x)$ along the cochlea. The damping parameter is $\zeta = -0.06$ (a) and $\zeta = 0.01$ (b).

Furthermore, this approximation of the feedback term is inaccurate. It does not take into account that the wave is decaying both to the left and to the right of its peak and hence a solution with smaller amplitude will be fed back. It also ignores the fact that the feed-forward mechanism changes the wave speed. We therefore proceed to study a model in which explicitly includes a spatial feed-forward term, instead of time-delay.

2C. **Feed-forward model.** Replacing the time delay in Equation (2-4) with a spatial delay of distance $\Delta(x)$ yields the feed-forward model. In some respect this is more physiological, but it still does not properly take into account the underlying source of the feed-forward term. The governing equation after expanding the solution into the form (2-3) becomes

$$\lambda^2\bar{p}(x) = \varepsilon^2\kappa_0(\lambda,x)\frac{\partial}{\partial x^2}\bar{p}(x) + \kappa_1(x)\frac{\partial}{\partial x^2}\bar{p}(x + \Delta(x)), \tag{2-9}$$

where $\kappa_0(\lambda, x) = \lambda^2 + 2\lambda\zeta(x)\omega_0(x) + \omega_0^2(x)$ and $\kappa_1(x) = \omega_0^2(x)\sigma(x)$. The excitation pattern compared to the time-delay model can be seen in Figure 2.1. With the obtained value of $\Delta(x)$ in Figure 2.2 we were not able to obtain a plausible result, which is already an indication that the derived relation in Equation (2-8) is inaccurate. Indeed, when looking for an exact value of distance $\Delta(x)$ and a constant $\hat{\sigma}$ that replaces the feedback coefficient σ, we find that $\Delta(x)$ and $\hat{\sigma}$ heavily depend on the stimulus frequency, and it is impossible to use fixed values for all frequencies. Nevertheless, we find from our simulations (indicated by dashed red lines in Figure 2.1) that a spatial delay of a quarter of the (inaccurately) estimated distance $\Delta(x)/4$ gives responses with the expected tall and broad peaks.

It can also be seen in Figure 2.1 that the feed-forward effect does not stabilize the model with negative damping and has less sharp tuning. However, with small positive damping the tuning is sharp and stability appears to be preserved. Note that stability in this context means only stability with respect to single frequency response. A more thorough stability analysis is outlined in the next section.

3. STABILITY

3A. **Stability of the delayed model.** Stability calculations for a delay equation can be demanding, depending on the type of the equation [19]. For delayed ordinary differential equations (DDEs) the problem reduces to finding roots of an exponential polynomial, followed by a check that all of these (typically infinitely many) roots have negative real part to ensure stability. In a numerical scheme one can count the number of unstable roots using the so-called argument principle [14]. The argument principle states that along a contour in the complex plane the argument variation of the function will be a constant times the difference between the number of poles and roots of the function inside the contour. This is very helpful, but only in the case that the function does not have poles.

Here we construct a function (the characteristic function) for the time-delayed cochlea model, whose roots determine the stability. However, since our underlying model is a delayed partial differential equation, it is not possible to guarantee that this function is without poles.

The construction of the characteristic function goes as follows. We say that λ is a characteristic root of Equation (2-4) if it has a non-trivial solution that satisfies the boundary conditions $\frac{\partial}{\partial x}\bar{p}(0) = 0$ and $\bar{p}(1) = 0$. Since Equation (2-4) is an ODE, one can solve it uniquely by specifying two boundary conditions $\bar{p}(0) = a_1$ and $\frac{\partial}{\partial x}\bar{p}(1) = a_2$. If for non-zero a_1 and a_2 the conditions $\frac{\partial}{\partial x}\bar{p}(0) = 0$ and $\bar{p}(1) = 0$ hold, there is a non-trivial solution and hence λ is a characteristic root.

One can therefore generate a characteristic matrix M such that

$$\begin{pmatrix} \frac{\partial}{\partial x}\bar{p}(0) \\ \bar{p}(1) \end{pmatrix} = M(\lambda) \begin{pmatrix} \frac{\partial}{\partial x}\bar{p}(1) \\ \bar{p}(0) \end{pmatrix}.$$

The left-hand-side of the above equation can only be zero for non zero right-hand side vector if $\det M(\lambda) = 0$. Hence, the roots of $\det M(\lambda) = 0$ are the characteristic roots of Equation (2-4). Since this is a delayed partial differential equation there may be a continuous spectrum, so finding the roots is a challenge. One can however approximate the roots by finding local maxima of the function $1/\det M(\lambda)$ that are above a certain threshold.

We solve the boundary value problem with a central finite difference scheme with 1200 equidistant points that is a rather fast and moderately accurate method. A plot of the roots can be seen in Figure 3.1, denoted by black dots. In the non-delay case, we can also approximate the roots by a (slower but more accurate) direct method using Chebyshev collocation to check the accuracy of our computation (denoted by yellow dots in Figure 3.1). We see that in the case
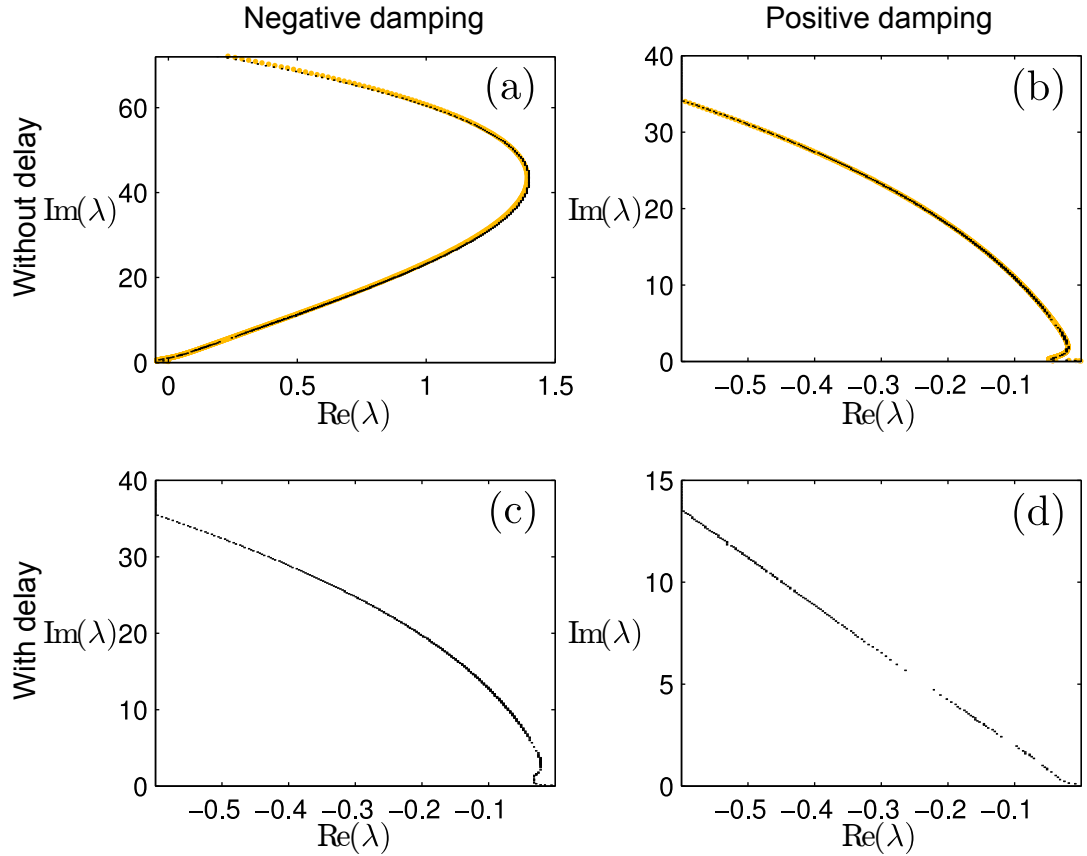
FIGURE 3.1. Stability of the time-delay model. Black points show the characteristic roots of Equation (2-4), computed from the characteristic function $\det M = 0$, without delay (panels (a) and (b)), and with delay (panels (c) and (d)). Panels (a) and (b) are computed without the delay term and the roots are also computed with the direct method of section 3B (yellow dots). The damping parameter is $\zeta_0 = -0.06$ for panels (a) and (c), and $\zeta_0 = 0.01$ for panels (b) and (d).

of negative damping ($\zeta_0 = -0.06$, shown in the left-hand column of Figure 3.1) adding time delay stabilizes the system. On the other hand, with positive damping ($\zeta_0 = 0.01$, shown in the right-hand column of Figure 3.1) the solution is always stable, with or without time-delay.

We note that both numerical methods provide spectra that are essentially indistinguishable in the case of no time-delay, which gives confidence in the accuracy of our computations. Furthermore, every root of our characteristic function is accompanied by a pole, therefore counting the difference between the number of roots and poles gives identically zero result, hence the argument principle cannot be used.

3B. **Stability of the feed-forward model.** The stability of the feed-forward model can be calculated more efficiently than that of the time-delay model. In order to formulate the spectral

problem we introduce the differential operators

$$D_0^2 \,:\, (D_0^2\varphi)(x) = \frac{\partial}{\partial x^2}\varphi(x)\ \varphi \in \{\phi \in C^2[0,1]\,:\,\frac{\partial}{\partial x}\phi(0) = 0,\ \phi(1) = 0\},$$

$$D_\Delta^2 \,:\, (D_\Delta^2\varphi)(x) = \frac{\partial}{\partial x^2}\varphi(x + \Delta(x))\ \varphi \in \{\phi \in C^2[0,1]\,:\,\frac{\partial}{\partial x}\phi(0) = 0,\ \phi(1) = 0\},$$

noting that the boundary conditions for Equation (2-9) are $\frac{\partial}{\partial x}\bar{p}(0) = 0$ and $\bar{p}(1) = 0$. The spectral problem is not an ODE any more, but is instead a neutral delay-differential equation. In contrast to the time-delay case the equation is polynomial in λ, and therefore can be transformed into a regular eigenvalue/eigenfunction problem:

$$\left[\begin{pmatrix} 0 & I \\ \varepsilon^2\omega_0^2\left(D_0^2 + \sigma D_\Delta^2\right) & 2\varepsilon^2\zeta\omega_0 D_0^2 \end{pmatrix} - \lambda \begin{pmatrix} I & 0 \\ 0 & I \end{pmatrix}\right]\begin{pmatrix} \psi_1 \\ \psi_2 \end{pmatrix} = \begin{pmatrix} 0 \\ 0 \end{pmatrix}. \qquad (3\text{-}1)$$

We discretize this boundary problem with Chebyshev collocation, using 2400 points, exactly as for the steady state solution, and put into an eigenvalue solver to obtain the spectrum.

The spectrum of Eq. 3-1 is shown in Figure (3.2). We see that the feed-forward mechanism
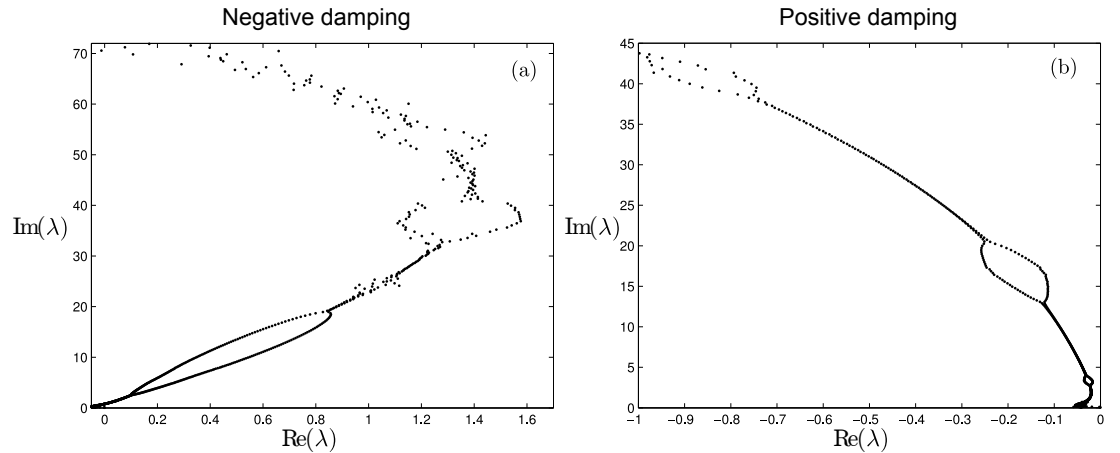

FIGURE 3.2. Characteristic roots of the feed-forward model (2-9). The damping parameter is $\zeta = -0.06$ (a) and $\zeta = 0.01$ (b).

does not stabilise the system with negative damping, but that stability is preserved with the combination of positive damping and spatial feed forward.

4. CONCLUSION

In this paper we have compared two cochlea models, one with time delay, and another with a spatial feed-forward mechanism. We calculated an approximate relation between the temporal and spatial delays and showed that no simple relation between the two such models can exist. Moreover, we found that the two models do not yield similar excitation profiles for equivalent physiological parameters. From a mathematical point of view, it is easier to control stability with a time-delay than with the feed-forward mechanism. In particular, we were not able to find a value for the feed-forward distance that made the model stable. However, the restriction on the damping does not restrict the sharpness of tuning with a stable model. In fact, with small positive damping one can achieve sharp tuning and qualitatively good agreement with data (also shown elsewhere [23]).

Furthermore, our stability analysis has given information on the alignment of the characteristic roots along the complex imaginary axis, which might also give insight into spontaneous otoacoustic emissions and even explain synchronization of the emitted frequencies. The distance of the roots from the imaginary axis might also indicate the sensitivity to different frequencies.

A natural next step that will be investigated in future work would be to introduce a nonlinear model for the outer hair cells themselves. Introduction of such a nonlinear term into the transmission line equations would enable us to investigate the effect of the loss of stability on the dynamics. More importantly, we would like to understand what kinds of local hair cell dynamics lead to compressive active nonlinearity when the spatial feedforward or temporal delay are taken into account. In particular, through matching with experimental data, this would enable us to gain a better global understanding of the relative importance of the longitudinal effects considered in this paper and the local hair cell dynamics.

Acknowledgements

References

[1] J. Ashmore. Cochlear outer hair cell motility. *Physiol. Rev.*, 88(1):173–210, JAN 2008.
[2] G. Békésy. *Experiments in Hearing.* McGraw Hill, 1960.
[3] P. Dallos. Cochlear amplification, outer hair cells and prestin. *Curr. Opin. Neurobiol.*, 18:370–376, 2008.
[4] H. Davis. An active process in cochlear mechanics. *Hear. Res.*, 9(1):79–90, 1983.
[5] V. M. Eguíluz, M. Ospeck, Y. Choe, A. J. Hudspeth, and M. O. Magnasco. Essential nonlinearities in hearing. *Phys. Rev. Lett.*, 84(22):5232–5235, 2003.
[6] B. Epp, J. L. Verhey, and M. Mauermann. Modeling the dynamics of the cochlea and its role in perception near threshold in quiet. *J. Acoust. Soc. Am.*, 2010. In press.
[7] C.D. Geisler. A realizable cochlear model using feedback from motile outer hair cells. *Hear. Res.*, 68:253–262, 1993.
[8] R. Ghaffari, Aranyosi A.J., and Freeman D.M. Longitudinally propagating traveling waves of the mammalian tectorial membrane. *Proc. Natl. Acad. Sci. USA*, 104(42):16510–16515, 2007.
[9] H. Helmholtz. *On the Sensation of Tone.* Dover Publications, 1863.
[10] A. Hubbard. A traveling-wave amplifier model of the cochlea. *Science*, 259(5091):68–71, 1993.
[11] A. J. Hudspeth. Making an effort to listen: mechanical amplification in the ear. *Neuron*, 59:503–545, 2008.
[12] K.D. Karavitaki and Mountain D.C. Evidence for outer hair cell driven oscillatory fluid flow in the tunnel of corti. *Biophys. J.*, 92(9):3284–3293, 2007.
[13] Marcia M. Mellado Lagarde, Markus Drexl, Victoria A. Lukashkina, Andrei N. Lukashkin, and Ian J. Russell. Determining the identity of the cochlear amplifier: electrical stimulation of the tecta mouse cochlea. In Cooper, NP and Kemp, DT, editor, *Concepts and challenges in the biophysics of hearing*, pages 106–112, PO BOX 128 FARRER RD, SINGAPORE 9128, SINGAPORE, 2009. Oticon Fdn; Otodynam Ltd; Starkey Lab Ltd; MED EL; Polytec GmbH; Tucker Davis Technol, WORLD SCIENTIFIC PUBL CO PTE LTD. 10th International Workshop on the Mechanics of Hearing, Staffordshire, ENGLAND, JUL 27-31, 2008.
[14] J. E. Marsden and Hoffman W. H. *Basic Complex Analysis.* W. H. Freeman, New York, 3rd edition, 1999.
[15] D. Ó'Maoiléidigh and F. Jülicher. The interplay between active hair bundle motility and electromotility in the cochlea, 2010.
[16] S. Puria and Steele C.R. Mechano-acoustical transformations. In *Handbook of the Senses*, pages 1–61. Draft, 2010.

[17] S. Ramamoorthy, N. V. Deo, and K. Grosh. A mechano-electro-acoustical model for the cochlea: Response to acoustic stimuli. *J. Acoust. Soc. Am.*, 121(5):2758–2773, MAY 2007.

[18] C. R. Steele and K. M. Lim. Cochlear model with three-dimensional fluid, inner sulcus and feed-forward mechanism. *Audiol. Neurootol.*, 4(3-4):197–203, 1999.

[19] G. Stépán. *Retarded dynamical systems: stability and characteristic functions.* Longman, London, 1989.

[20] R. Szalai, D. Ó'Maoiléidigh, H. Kennedy, N.P. Cooper, and M. Homer. On the origins of the compressive cochlear nonlinearity. *J. Acoust. Soc. Am.*, 2010. In preparation.

[21] J. Tinevez, F. Jülicher, and P. Martin. Unifying the various incarnations of active hair-bundle motility by the vertebrate hair cell. *Biophys. J.*, 93(11):4053–4067, 2007.

[22] L. N. Trefethen. *Spectral Methods in MATLAB.* SIAM Philadelphia, 2000.

[23] Y. Yoon, S. Puria, and C.R. Steele. A cochlear model using the time-averaged Lagrangian and the push-pull mechanism in the organ of corti. *J. Mech. Matl. Struct.*, 4(5):977–986, 2009.

[24] G. Zweig. Finding the impedance of the organ of corti. *J. Acoust. Soc. Am.*, 89:1229–1254, 1991.

E-mail address: [1]`r.szalai@bristol.ac.uk`

[1,3,4]Bristol Centre for Applied Nonlinear Mathematics, Department of Engineering Mathematics, University of Bristol, Bristol BS8 1TR, United Kingdom, [2]Carl von Ossietzky Universität Oldenburg, Institute of Physics, Neuroacoustics, Carl-von-Ossietzky-Str. 9-11, 26111 Oldenburg, Germany.